Bioconjugate Chemistry

Article

pubs.acs.org/bc

PESIN Multimerization Improves Receptor Avidities and *in Vivo* Tumor Targeting Properties to GRPR-Overexpressing Tumors

Simon Lindner,[†] Christina Michler,[†] Björn Wängler,[‡] Peter Bartenstein,[†] Gabriel Fischer,[†,§] Ralf Schirrmacher,[∥] and Carmen Wängler*[,†,§]

[†]Department of Nuclear Medicine, University Hospital Munich, Ludwig Maximilians-University Munich, 81377 Munich, Germany
[‡]Molecular Imaging and Radiochemistry and [§]Biomedical Chemistry, Department of Clinical Radiology and Nuclear Medicine, Medical Faculty Mannheim of Heidelberg University, Theodor-Kutzer-Ufer 1-3, 68167 Mannheim, Germany
[∥]McConnell Brain Imaging Centre, Montreal Neurological Institute, McGill University, Montreal, Quebec H3A 2B4, Canada

ABSTRACT: The gastrin releasing peptide receptor (GRPR), being overexpressed on several tumor types, represents a promising target for specific noninvasive *in vivo* tumor imaging using positron emission tomography. Many of the radiolabeled bombesin analogs being applied in tumor imaging, however, suffer from shortcomings such as limited *in vivo* stability and poor tumor to background ratios. These obstacles can be overcome by peptide multimerization, as this approach results in constructs comprising several copies of the same peptide, thus retaining the ability to specifically bind to the target structure even if one peptide is cleaved. Furthermore, peptide multimers can result in increased binding avidities to the target, which can entail higher absolute tumor uptakes and also tumor to background levels. We therefore synthesized monomers and multimers of the peptide PESIN on dendrimer scaffolds comprising linkers of different lengths. The monomers/multimers were functionalized with the chelator NODAGA, efficiently radiolabeled with ^{68}Ga and evaluated *in vitro* regarding their GRPR binding affinity. The results show that shorter distances between the peptide moieties result in substantially higher binding affinities/avidities of the monovalent/multivalent PESIN ligands to the GRPR. Furthermore, the bivalent ligands gave the best results in terms of binding avidity, achieving a 2.5-fold increase in avidity compared to the respective monomer. Moreover, the most potent bivalent ligand showed an about 2-fold higher absolute tumor uptake and twice as high tumor-to-background ratios than the monomeric reference DOTA-PESIN in an initial animal PET study in tumor-bearing mice. Thus, besides high avidities, multivalency also positively influences the *in vivo* pharmacokinetics of peptide multimers.

INTRODUCTION

The gastrin-releasing peptide receptor (GRPR) which belongs to the bombesin receptor family is overexpressed on a variety of tumors such as prostate, breast and colon carcinomas, small cell lung cancer, gastrinomas, and head and neck tumors.[1−3] Thus, this receptor represents a promising target structure for the early diagnosis and localization of these tumor types, as well as for the monitoring of treatment response and recurrent disease with molecular imaging techniques such as positron emission tomography (PET).

For these applications, radiolabeled ligands are required that are able to bind to the GRPR with high affinity enabling a high tumor uptake of the radiotracer.[4−6] Since the natural ligand bombesin exhibits a limited *in vivo* stability, different agonistic and antagonistic peptide analogs binding to the GRP receptor have been developed for application in PET imaging over the last years.[7−16] However, most of these analogs suffer from shortcomings regarding their biodistribution properties such as low *in vivo* stabilities and thus short plasma half-lives, fast excretion, high background, or low tumor uptakes.[7,12,13,16−18] Nevertheless, promising candidates were developed recently that could provide a basis for the design of bombesin analogs able to overcome these limitations.[7,14,15,17,19,20] One possible strategy to further improve the pharmacokinetic properties of bombesin derivatives and to address the mentioned obstacles is the multimerization of GRPR-affine peptides, as this can result in compounds exhibiting improved *in vitro* and *in vivo* properties compared to the respective monomers. Multimerization of cRGD peptides was, e.g., shown to result in improved avidities to the target integrin $\alpha_v\beta_3$, increased plasma half-lives, higher tumor uptakes, improved tumor-to-background ratios, as well as prolonged tumor retention compared to monomeric peptides.[21−23]

These favorable effects can be attributed to a more probable rebinding of the ligand to its receptor in the case of dissociation and a higher local ligand concentration in direct vicinity to the receptor together with a possible concomitant binding of peptide moieties of the multimer to different receptors on the same cell. The scaffold and linker structures applied in such multi-

Received: October 7, 2013
Revised: February 15, 2014
Published: February 17, 2014

dx.doi.org/10.1021/bc4004662 | *Bioconjugate Chem.* 2014, 25, 489−500

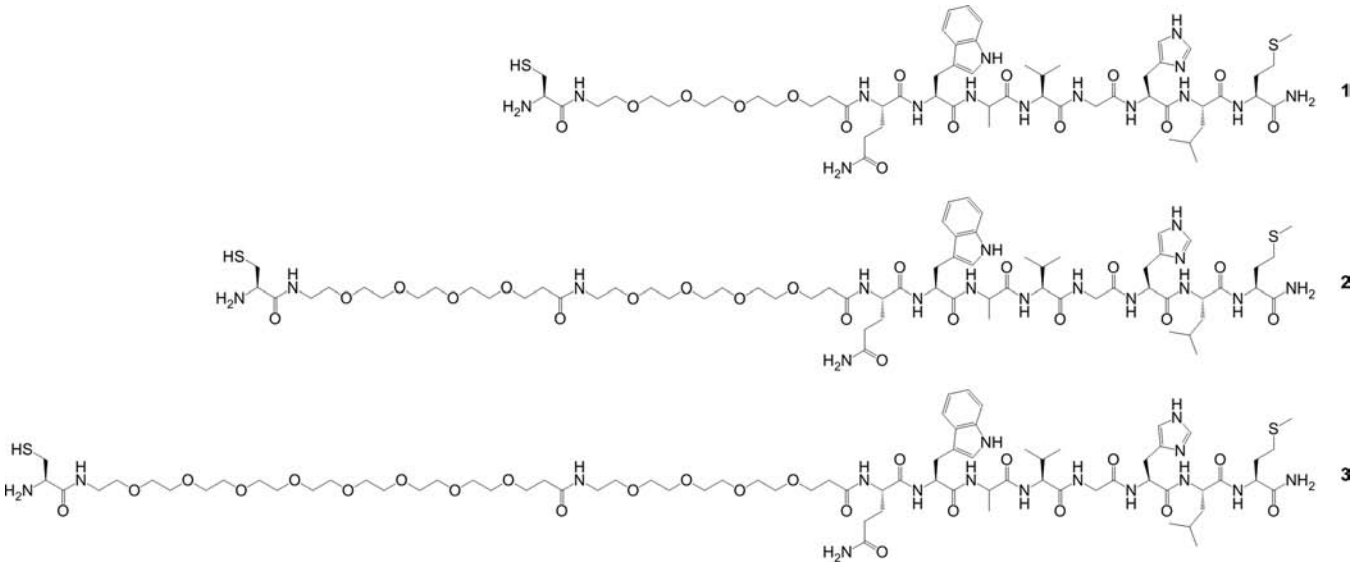

Figure 1. Structures of the PESIN derivatives **1**−**3** used in the multimerization reactions.

merization reactions have to be of sufficient length to enable a concomitant binding of peptide moieties. At the same time, they have to be short enough to not impose a high entropic cost which limits the enthalpic gain of ligand binding, the probability of simultaneous binding, as well as the local concentration of the ligand in direct vicinity to the target receptor.

Due to the expected favorable properties such as improved avidities, higher *in vivo* tumor accumulation, and improved tumor retention characteristics compared to the respective monomers, earlier and also very recent approaches aimed at the synthesis of bivalent bombesin analogs.[24−29] So far, the obtained results were, however, not optimal, showing mostly decreased and at best comparable *in vitro* binding affinities of monomers and dimers most probably due to nonoptimized distances between the peptide moieties of the dimers.

Hence, it was suggested recently that the application of longer linker structures between adjacent peptide moieties could result in more favorable binding parameters of the bivalent ligands.[24]

Furthermore, only bivalent bombesin analogs were synthesized so far most probably due to the intricate synthesis of larger, well-defined constructs, although the *in vivo* tumor targeting properties might strongly profit from linkage of more than just two peptide moieties, as has been shown before for other peptides.[4,30]

Regarding the limited available information about multivalent bombesin analogs, we intended to systematically investigate the influence of the number of peptide moieties per multivalent system as well as the distance between adjacent peptide entities on the achievable binding avidities of multivalent GRP receptor ligands. As—among the available agonists for diagnostic GRPR PET imaging—PESIN is one of the most promising ligands due to tolerable *in vivo* stability and reasonable tumor uptake, PESIN was used as the GRPR-affine peptide for this multimerization approach. By this, we aimed to determine structure−activity relationships for multivalent PESIN constructs and to identify promising directions for further developments that are expected to result in the efficient *in vivo* PET imaging of GRPR overexpressing tumors.

RESULTS AND DISCUSSION

Over the past years, several peptide agonists and antagonists targeting the GRPR have been developed for application in PET imaging of GRP receptor overexpressing tumors.[7−12,17] Among these, the agonist PESIN has attracted attention as it combines favorable properties such as tolerable *in vivo* stability and reasonable tumor uptake, as well as tumor to background ratios.[7,17] Hence, it is one of the most promising available agonists for diagnostic GRPR PET imaging. Consequently, PESIN was chosen as the peptidic GRPR-binding part for peptide multimerization. Usually, small peptides are preferred for imaging purposes as they exhibit a fast clearance and are not prone to enhanced permeability and retention (EPR) effects. However, when dealing with sensitive physiological peptides, the artificial structure and enhanced molecular size of the peptide multimers can result in a higher metabolic stability as well as decelerated blood clearance compared to the respective monomers. These effects can enhance the interaction probability of multivalent peptide ligands with the target receptor, resulting in a more favorable *in vivo* tumor targeting as well as improved tumor accumulation properties of the multimers as compared to the monomers.[32−34]

For the synthesis of the multivalent PESIN ligands, PAMAM (polyamidoamine) dendrimers were used as scaffold structures, as they allow for the synthesis of highly homogeneous and symmetrical multimerization products with constant distances between adjacent peptide moieties.[35]

Regarding the structural design of the multimers, the choice of an appropriate linker length is also important in order to enable high avidities of the multimeric constructs. This was shown in previous attempts to develop bivalent bombesin analogs exhibiting short linkers, resulting in decreased avidities of the dimers compared to the monomeric systems.[25,27] However, very long linkers also were shown to have a negative influence on the binding properties of bivalent bombesin analogs.[28] Hence, to systematically optimize our compound library, we used linkers of different lengths in our multimer syntheses to elucidate the influence of linker lengths on the achievable binding avidities to the GRPR. As the PESIN sequence itself comprises a PEG_3-linker structure, we synthesized sets of PESIN monomers, dimers, tetramers, and octamers using either no additional linker

dx.doi.org/10.1021/bc4004662 | *Bioconjugate Chem.* 2014, 25, 489−500

Scheme 1. (A) Synthesis of NODAGA-Derivatized PESIN Monomers 20−22 and Multimers 23−31.[a] (B) Schematic Depiction of Synthesized PESIN Monomers 20−22, Dimers 23−25, Tetramers 26−28, and Octamers 29−31

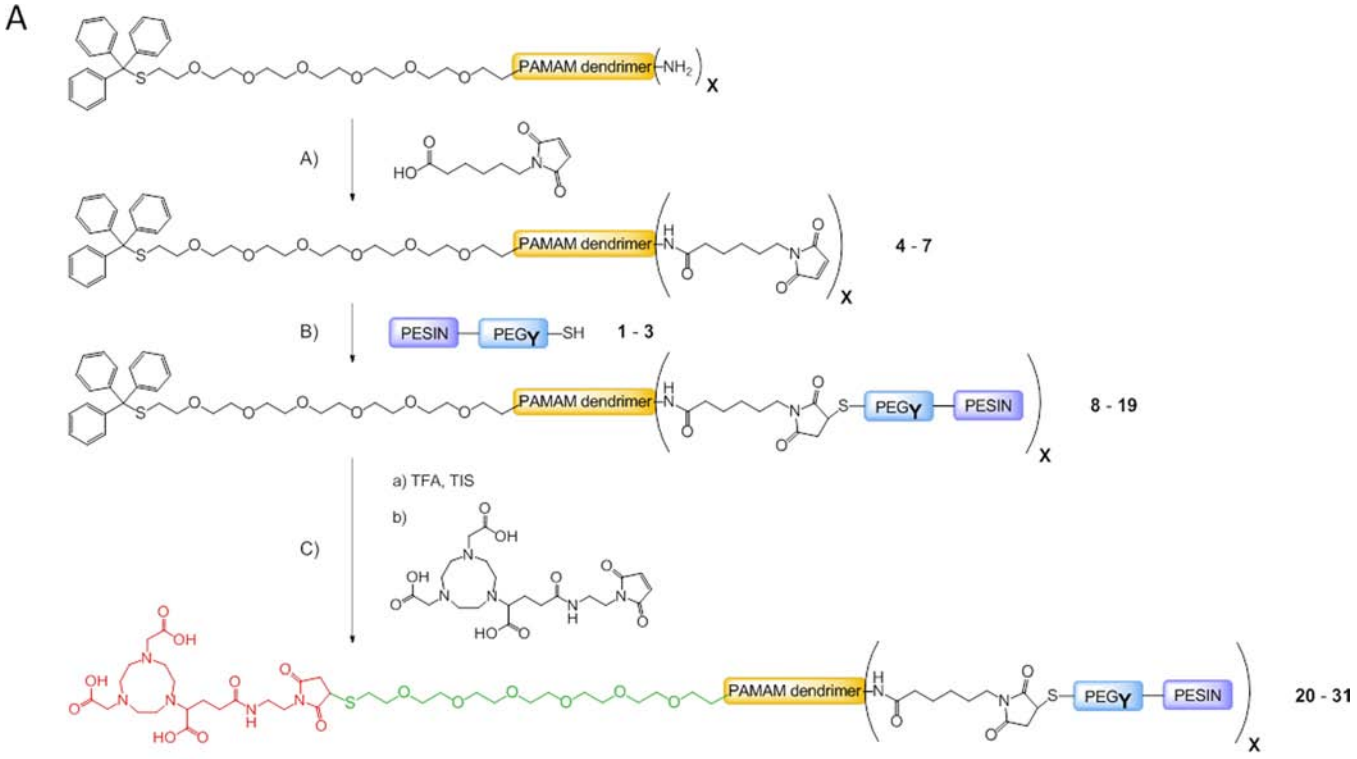

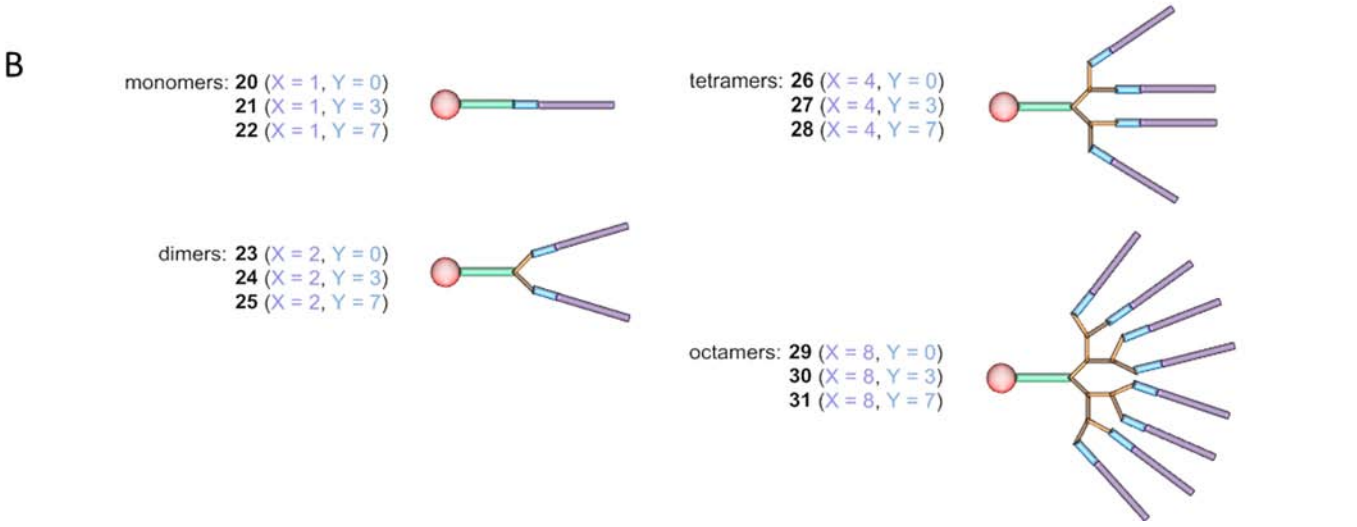

[a]Conditions: (A) PyBOP, DIPEA, DMF, RT, 1 h, yields: 46−67%; (B) phosphate buffer/MeCN, pH 6.9-7.2, RT, 2−60 min, yields: 73−87%; (C) (*i*) TFA:TIS 40:1, RT, 5 min, (*ii*) H_2O:MeCN 1:1, pH 6.9−7.2, RT, 2−10 min, yields: 45−79% over both steps.

structure or an additional PEG_3 or PEG_7-linker, resulting in distances between two adjacent peptides within the multivalent ligands of 74, 106, and 130 bond lengths, respectively.

In order to obtain homogeneous peptide multimers, a highly efficient conjugation chemistry is required that enables the synthesis of uniformly derivatized and peptide-loaded dendritic scaffolds. The Michael addition of thiols to maleimides gives very favorable results in peptide multimerization compared to other chemoselective conjugation reactions such as oxime and triazole formation.[35] This reaction type was therefore used for the conjugation of peptides to the dendritic core structures.

Synthesis of Functionalized PESIN Analogs. The PESIN monomers **1**−**3** (Figure 1) that were used in the multimerization reactions were synthesized by standard Fmoc-based solid phase peptide synthesis (SPPS) by successive conjugation of the respective amino acids to a rink amide resin using standard reaction conditions.[35−37]

The introduction of PEG linkers was accomplished by derivatization of PESIN on solid support as this approach is much more feasible than the conjugation of the PEG linkers to the dendritic scaffold structures and their subsequent derivatization with PESIN. The PESIN-PEG_X sequences were further functionalized on solid support with cysteine in order to obtain

dx.doi.org/10.1021/bc4004662 | *Bioconjugate Chem.* 2014, 25, 489−500

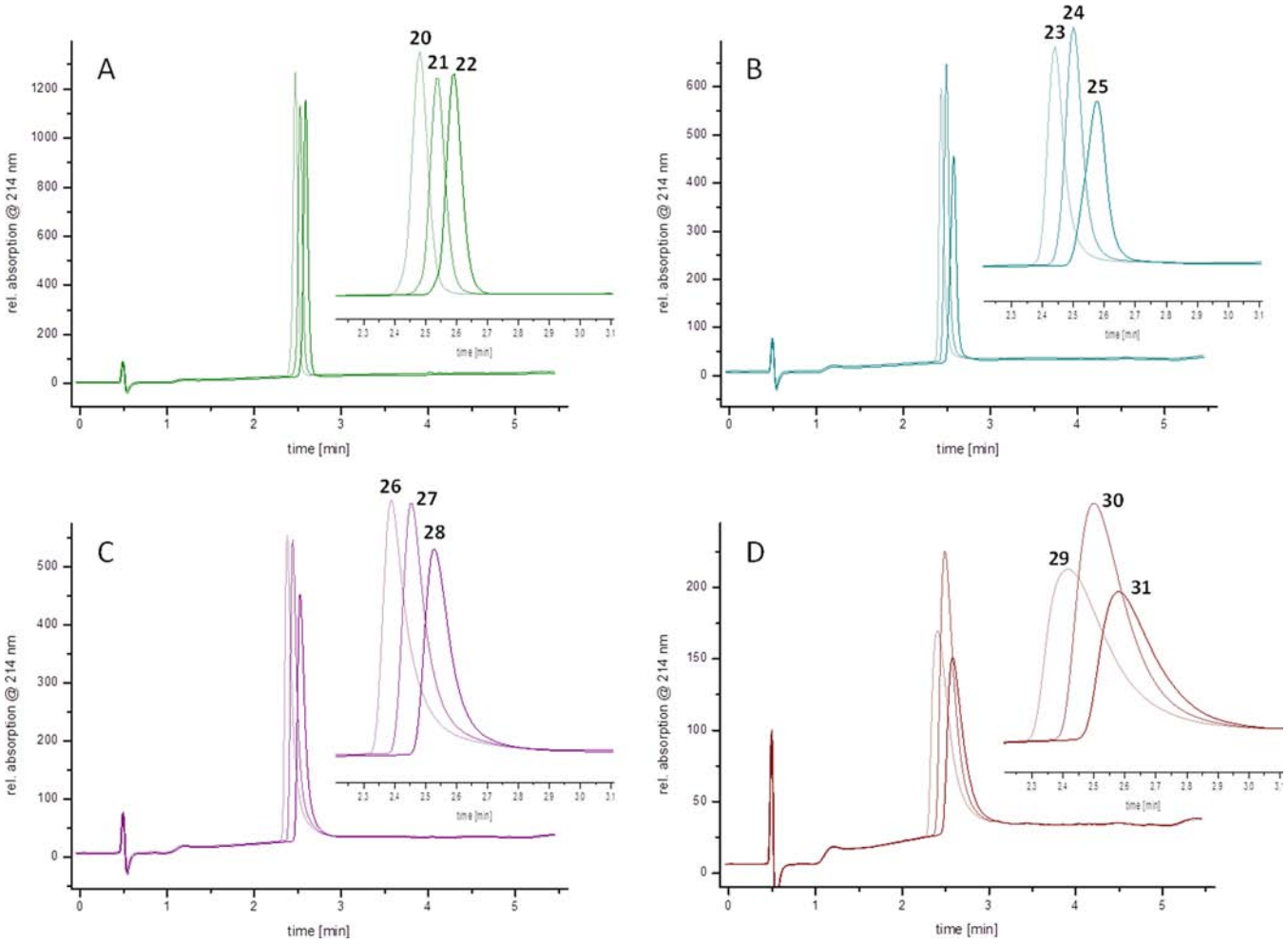

Figure 2. Analytical HPLC chromatograms of the purified NODAGA-functionalized PESIN monomers/multimers obtained using the same HPLC conditions, showing a significant product peak broadening correlating with molecular size: (A) monomers **20**–**22**, (B) dimers **23**–**25**, (C) tetramers **26**–**28**, (D) octamers **29**–**31**.

an *N*-terminal thiol functionality amenable to dendrimer conjugation via Michael addition.

The products Cys-PESIN (**1**), Cys-PEG_3-PESIN (**2**), and Cys-PEG_7-PESIN (**3**) were obtained in yields of 44% to 60% after cleavage from the resin, HPLC purification, and lyophilization and were consecutively used in the multimerization reactions with the maleimide-derivatized dendritic scaffolds **4**–**7** (Scheme 1A).

Synthesis of Chelator-Comprising Peptide Monomers/Multimers 20–31, ^{68}Ga-Radiolabeling and Determination of Serum Stability. PAMAM dendrimers (built on the basis of an *S*-trityl-protected amino-functionalized PEG_5 linker[31]) were synthesized as symmetrical and spherical scaffold structures for peptide multimerization, resulting in a linear monomer and small dendrimers containing two, four, and eight amino functionalities for further derivatization. The PEG_5 linker was applied as the basis for the PAMAM dendrimer synthesis as it allows for the efficient introduction of a chelating agent in the last synthesis step despite the sterically demanding dendritic multimer structures. These scaffold PAMAM dendrimers were in the following derivatized with maleimido hexanoic acid, resulting in maleimide-monomer to -octamer **4**–**7** (Scheme 1A).

After HPLC purification, these maleimide-functionalized dendrimers (**4**–**7**) were reacted in a Michael addition reaction at neutral pH with the PESIN derivatives **1**–**3** to the respective *S*-trityl-protected PESIN monomers **8**–**10** and multimers **11**–**19** within 2 to 60 min at ambient temperature (Scheme 1A).

Regarding the solubility and purification of these protected peptide monomers and multimers (**8**–**19**), some trends were observed that interestingly did not recur for the final chelator-conjugated products **20**–**31**. It was, for example, found that for monomers and multimers **8**–**19**, an increasing PEG linker length resulted in a significantly enhanced solubility. Among the different size classes, the dimers **11**–**13** interestingly showed the least solubility at neutral pH, whereas it increased in the case of the smaller monomers (**8**–**10**) and larger tetramers and octamers (**14**–**19**). The purification of the products was usually performed by semipreparative HPLC using 0.1% formic acid (FA) as an additive to the HPLC solvents. In contrast to trifluoroacetic acid (TFA), which is the commonly used acidic additive, FA does not impede a successful ESI mass spectrometry characterization of the products. However, the protected octamers **17**–**19** required TFA instead of FA as HPLC solvent additive during purification for a successful peak separation, but in the following prevented characterization of the products by ESI. Thus, these three compounds were further reacted to the final chelator-comprising products **29**–**31** and successfully identified by final ESI mass spectrometry.

In the following, the *S*-trityl protecting group of the monovalent/multivalent PESIN ligands **8**–**19** was removed by

dx.doi.org/10.1021/bc4004662 | *Bioconjugate Chem.* 2014, 25, 489–500

reaction with TFA and triisopropylsilane (TIS) within 5 min at ambient temperature. After evaporation of TFA and TIS, the crude products were redissolved in a mixture of water and acetonitrile and reacted with NODAGA-maleimide after adjusting the pH to 6.9 to 7.2, yielding the chelator-functionalized PESIN monomers **20**−**22** and multimers **23**−**31** (Scheme 1A and B).

For final ^{68}Ga-radiolabeling, the chelator NODAGA (1,4,7-triazacyclononane-1-glutaric acid-4,7-diacetic acid) was preferred over the more common chelator DOTA (1,4,7,10-tetraazacyclododecane-1,4,7,10-tetraacetic acid) as NODAGA allows for the stable and efficient complexation of $^{68}Ga^{3+}$ at ambient temperature.[38,39] Furthermore, it forms stable complexes not only with $^{68}Ga^{3+}$, but also with $^{64}Cu^{2+}$.[40,41] This could be especially favorable if *in vivo* imaging at late time-points post injection was required due to a possibly slow biodistribution of the large multimers as ^{64}Cu exhibits a longer half-life of 12.7 h than ^{68}Ga ($t_{1/2}$ = 68 min).

The conjugation reactions of the PESIN derivatives **1**−**3** to the maleimido-functionalized PAMAM dendrimer cores **4**−**7** proceeded efficiently within short reaction times, giving the homogeneously derivatized dendritic structures. Also, the subsequent deprotection and maleimide−NODAGA conjugation reactions yielding the final products **20**−**31** were not impeded by the sterically demanding multivalent structures.

However, moderate recovery rates were found for tetramers (**26**−**28**) and especially octamers (**29**−**31**) after HPLC purification. This can be attributed to their large molecular size resulting in an increasing interaction with the monolithic column material which is reflected in a significant broadening of the product peaks with increasing molecular size (Figure 2). However, as the reactants exhibit considerably differing elution profiles, the HPLC purification of the products could nevertheless be successfully accomplished despite the observed significant peak broadening.

Finally, the PESIN monomers/multimers **20**−**31** were successfully radiolabeled with ^{68}Ga. The ^{68}Ga-labeling was performed using the fractioned elution method of ^{68}Ge/^{68}Ga generators,[42] avoiding a prereaction purification of the generator eluate. Using the chelator NODAGA instead of DOTA enables a simplified radiolabeling protocol which does not require a heating step for complexation of the radiometal allowing for a very efficient labeling reaction at ambient temperature within 10 min.[39] The ^{68}Ga-labeled products [^{68}**Ga**]**20** − [^{68}**Ga**]**31** could be obtained in high radiochemical yields and purities of 96−99% as well as specific activities of 19 to 28 GBq/μmol starting from 170−290 MBq of $^{68}Ga^{3+}$. For *in vivo* studies, higher ^{68}Ga starting activities of ∼800 MBq were used, resulting in specific activities of up to 79 GBq/μmol which is adequate for *in vivo* PET tumor imaging applications.

In order to prove a sufficient stability of the ^{68}Ga-labeled substances for an *in vivo* application, we exemplarily studied the *in vitro* stability of tetramer [^{68}**Ga**]**26** in human serum. For this purpose, **26** was labeled with 270−290 MBq of ^{68}Ga, added to human serum and incubated at 37 °C for up to 4 h. At appropriate time-points (1, 2, 3, and 4 h), aliquots were taken, serum proteins were precipitated with acetonitrile at 0 °C, precipitate and supernatant were measured for radioactivity to exclude the possibility of product or side-product precipitation and the supernatant was analyzed by HPLC. In Figure 3, the analytical radio-HPLC chromatograms of [^{68}**Ga**]**26** directly after radiolabeling and incubation for 1, 2, 3, and 4 h in serum are given, showing a liberation of approximately 1% of the ^{68}Ga from

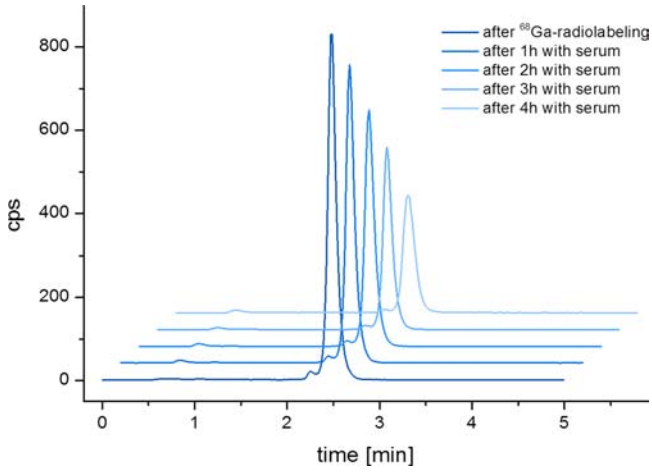

Figure 3. Analytical radio-HPLC chromatograms of [^{68}**Ga**]**26** directly after radiolabeling and incubation for 1, 2, 3, and 4 h in human serum at 37 °C.

the NODAGA complex over time. However, no fragmentation of the peptide multimer was observed, indicating an excellent stability of the synthesized monovalent/multivalent substances for an *in vivo* use.

***In Vitro* Binding Affinity/Avidity Evaluation of Peptide Monomers/Multimers 20−31 on PC-3 Cells.** The synthesized monomers **20**−**22** and multimers **23**−**31** were evaluated in a competitive binding assay by displacement of ^{125}I-[Tyr^4]-bombesin on the human prostate carcinoma PC-3 cell line. By this, we intended to assess the effects of linker lengths and the number of peptide moieties on the achievable binding affinities/avidities of the monomers/multimers. Natural bombesin was coevaluated as internal standard and showed an IC_{50} value of 0.89 ± 0.14 nM which is in accordance with literature data.[8] In Figure 4, the binding curves and the results of these *in vitro* evaluations are summarized.

From these results, different trends can be observed regarding the influence of molecular design on the binding parameters of the resulting multivalent PESIN ligands.

First and most obvious, the effect of binding avidities increasing proportionally to the number of peptide moieties—as has been found in the case of integrin $\alpha_v\beta_3$-binding cRGD multimers[35]—was not observed in the case of these PESIN multimers. In contrast, an avidity optimum was determined—irrespective of the linker structure used—for the group of dimeric substances which exhibited the highest binding avidities of the tested multivalent PESIN ligands. This effect might be attributable to a potential lack of receptor clustering as observed in the case of $\alpha_v\beta_3$ integrin upon cRGD peptide binding. A missing receptor clustering would consequently on average result in a concomitant binding of at most two peptide entities, limiting the contribution of any additional peptide moieties within the multimer to the overall binding avidity of the system, and would furthermore result in an even negative influence of further peptide moieties due to steric hindrance and higher entropic cost. These assumptions of missing GRP receptor clustering and concomitant binding of at most two peptide moieties of the multimers are further corroborated by looking at receptor densities: $\alpha_v\beta_3$ integrin is expressed in lower density on U87MG cells ($(1.28 \pm 0.46) \times 10^5$ receptors/cell)[43] than GRPR on PC-3 cells ($(2.7 \pm 0.1) \times 10^6$ receptors/cell).[44] Nevertheless, cRGD peptides—usually tested on U87MG cells for avidity—were

dx.doi.org/10.1021/bc4004662 | *Bioconjugate Chem.* 2014, 25, 489−500

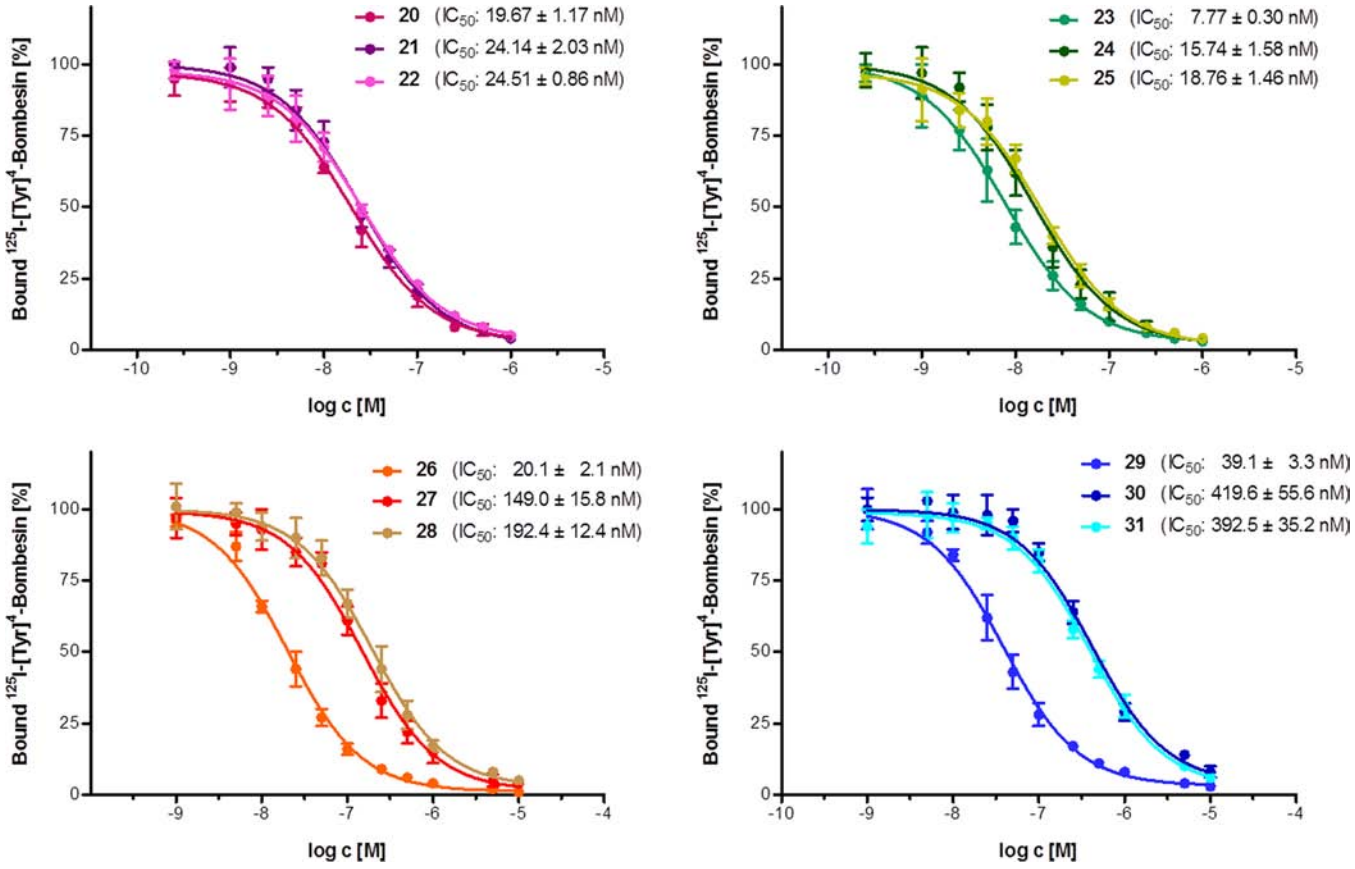

Figure 4. Binding curves and IC_{50} values for chelator-comprising monomers and multimers **20**−**31** obtained from the competitive binding experiments on human prostate carcinoma PC-3 cells. Results were obtained from at least three independent experiments each performed in triplicate.

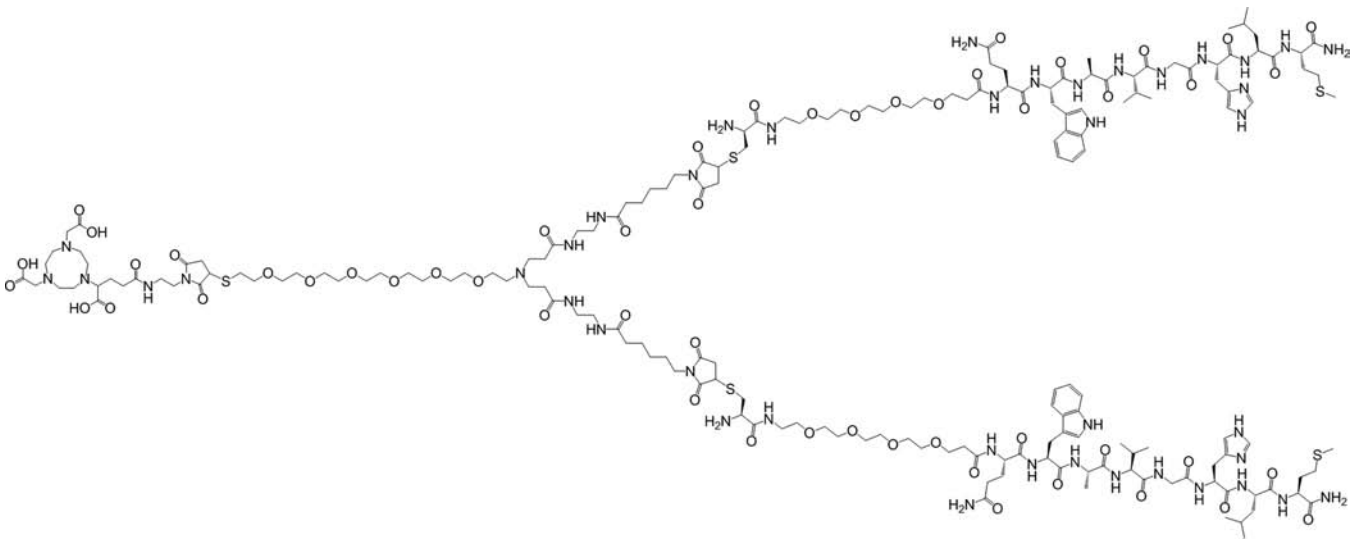

Figure 5. Structure of the most potent of the tested substances NODAGA-$PESIN_2$ (**23**).

often shown to strongly profit from multimerization exhibiting higher avidities with increasing number of peptide moieties.

Thus, the observed avidity enhancement of bivalent bombesin analogs seems mostly to be a result of an increased local ligand concentration at the receptor and thus a higher probability of binding and also rebinding in the case of dissociation from the receptor (multivalency effect) and only to a minor extent to be related to a simultaneous binding to adjacent receptors on the same cell, although the structural changes resulting from dimerization might also have an influence on avidities. For any future developments in the field of multivalent bombesin analogs, bivalent compounds should have the highest potential to exhibit optimized GRPR binding properties.

The other parameter strongly influencing the binding avidities of the multimers relates to the applied linker lengths resulting in different distances between adjacent peptide moieties. The introduction of additional PEG_X linkers—apart from the PEG_3 linker already present within the PESIN sequence—substantially

dx.doi.org/10.1021/bc4004662 | Bioconjugate Chem. 2014, 25, 489−500

decreases the binding affinities/avidities of the monovalent and multivalent ligands to the GRPR (Figure 4). This effect can be observed within the subset of monomers, dimers, tetramers, and octamers but is significantly more pronounced within the group of tetramers **26**−**28** and octamers **29**−**31**. This could be a consequence of the strongly increased entropy which is a result of the increased molecular flexibility in these systems. This high entropic cost limits the enthalpic gain of ligand-to-receptor binding, decreases the ligand concentration in direct vicinity to the target receptor, and thus reduces the interaction probability of the nonbound peptide moieties with the GRPR. In summary, the best results were found within each group (monomers to octamers) for the compound comprising the shortest linker, resulting in minimal distances between two adjacent peptide moieties of 74 bond lengths.

Taking the literature context into account, it can be inferred that, in the multimerization of bombesin analogs, multivalent constructs should exhibit a minimal distance between adjacent peptides of between 28 bond lengths (which were shown before to result in an at least slightly increased avidity compared to the respective monomer[24]) and 74 bond lengths (that were found in this study to result in a significantly 2.5-fold increased avidity compared to the monomer).

Thus, among the synthesized monovalent and multivalent PESIN ligands, the compound showing the highest GRPR binding avidity is the PESIN dimer **23** (Figure 5).

This is the first example of a bivalent bombesin analog (**23**) exhibiting a significantly increased binding avidity of 7.8 nM compared to its corresponding monomer (**20**) showing an affinity of 19.7 nM.

This relevant avidity enhancement together with the fact that peptide multimerization itself is able to positively influence *in vivo* pharmacokinetics[45] is expected to result in improved *in vivo* tumor accumulation properties of the bivalent compound **23** compared to a respective monomer.[22,46,47]

***In Vivo* Evaluation of the Most Potent Bivalent Ligand 23 in PC-3 Tumor-Bearing Mice.** In order to prove this assumption, we initially evaluated the most promising bivalent compound [^{68}**Ga**]**23** in PC-3 tumor-bearing mice in direct comparison to ^{68}Ga-DOTA-PESIN as the monomeric gold-standard. If the binding avidity to the GRPR alone was the critical criterion for tumor targeting and accumulation, ^{68}Ga-DOTA-PESIN might give superior *in vivo* results as it was shown to exhibit a slightly higher receptor binding affinity of 6.6 ± 0.1 nM.[19] If, however, the bivalency were also able to positively influence the resulting *in vivo* pharmacokinetics, **23** should give comparable or even superior *in vivo* animal PET imaging results despite the slightly lower affinity of 7.7 ± 0.3 nM. In Figure 6 and 7 as well as Table 1, the results of these initial *in vivo* evaluations of [^{68}**Ga**]**23** in comparison to the reference ^{68}Ga-DOTA-PESIN are shown.

As can be deduced from the *in vivo* data, the bivalent compound [^{68}**Ga**]**23** exhibits a higher absolute kidney uptake than the monomeric ^{68}Ga-DOTA-PESIN, as well as a prolonged retention in this organ, which is reflected in the low tumor-to-kidney ratios for both tracers being even more pronounced in the case of [^{68}**Ga**]**23** (Table 1, Figure 7D). This effect of increased kidney accumulation resulting from peptide multimerization, which was also often observed for other peptide dimers and tetramers before,[21−23,32] can be attributed to an increased tubular reabsorption of the peptide multimers compared to the respective monomers and is assumed to be a result of the increased positive charge of the larger constructs.

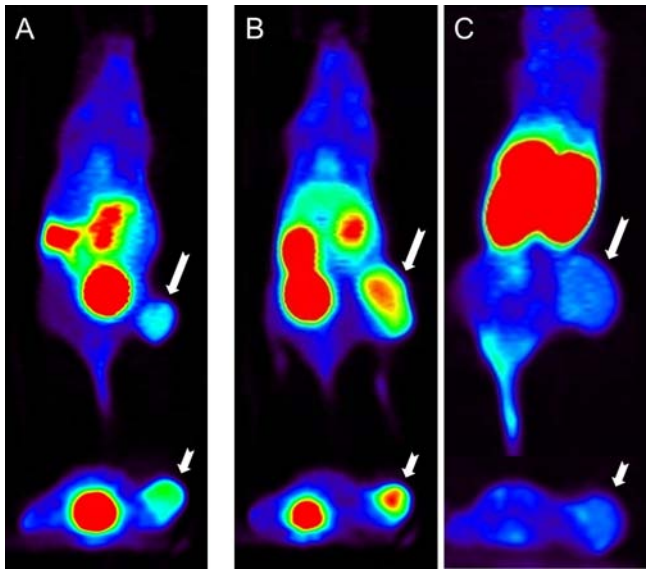

Figure 6. Coronal (upper row) and transaxial (lower row) cut of 120 min sum animal PET images of ^{68}Ga-DOTA-PESIN (A) which was taken as the reference and ^{68}Ga-NODAGA-PESIN$_2$ ([^{68}**Ga**]**23**) (B) in PC-3 tumor-bearing mice; (C) shows the blocking experiment for [^{68}**Ga**]**23**, using bombesin as the blocking substance. Each compound was evaluated in four animals, exhibiting tumors of comparable size. White arrows indicate tumors.

Apart from this observed higher kidney uptake, [^{68}**Ga**]**23** exhibits improved tumor-binding properties as compared to the monomeric reference ^{68}Ga-DOTA-PESIN with about twice as high tumor-to-background ratios (Figure 7A, the background value is obtained from the activity of the whole mouse, including all organs) and about 2-fold higher absolute tumor uptakes (Figure 7B), resulting in a more favorable and GRPR-specific *in vivo* tumor visualization of the dimer compared to the monomer (Figure 6). Interestingly, the dimer also shows a much faster blood clearance than the monomer (Table 1) contributing to the obtained favorable imaging results.

Compared to other described examples of preclinically evaluated bivalent bombesin analogs which showed moderate tumor and high nontarget organ accumulations despite promising *in vitro* binding affinity data,[24,29] [^{68}**Ga**]**23** shows a higher tumor accumulation and higher tumor-to-background ratios than the monomeric reference .

Hence, taking these results and the literature data into account, it can be concluded that not only do binding affinities/avidities give a valid indication of *in vivo* tumor binding properties, but also bivalency itself contributes obviously very favorably to *in vivo* pharmacokinetics of multivalent peptides. Further developments of dimeric GRPR-binding peptides, optimizing the distance between both peptide moieties, could result in even more favorable *in vivo* pharmacokinetic properties of the resulting peptide dimers.

■ CONCLUSIONS

The herein presented chemistry and systematic *in vitro* evaluation of synthesized monovalent and multivalent PESIN ligands give valuable insights into structure−activity relationships of bombesin analog multimers. It was shown that in contrast to the results obtained in former studies, the multimerization of bombesin analogs can result in compounds

dx.doi.org/10.1021/bc4004662 | *Bioconjugate Chem.* 2014, 25, 489−500

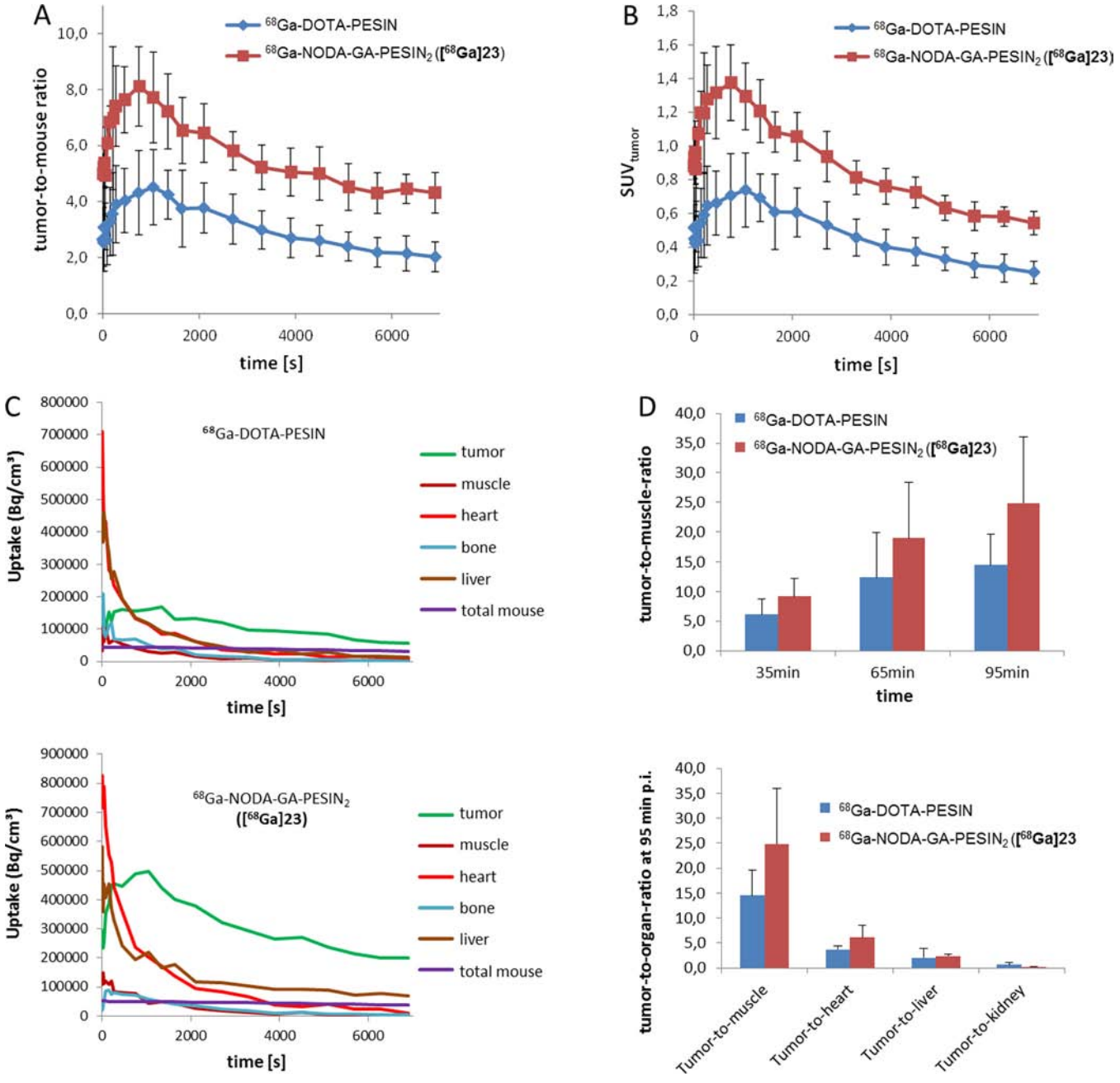

Figure 7. *In vivo* tumor-to-background ratios (A) and absolute tumor uptakes (B) over time as well as time−activity curves for selected organs (C) and tumor-to-organ ratios of both tracers (D).

Table 1. Tumor-to-Organ Ratios for Different Time-Points Obtained from the in Vivo Animal PET Data for ^{68}Ga-DOTA-PESIN and ^{68}Ga-NODAGA-PESIN$_2$ ([^{68}Ga]23)

	^{68}Ga-DOTA-PESIN				^{68}Ga-NODAGA-PESIN$_2$ ([^{68}Ga]23)			
time-point p.i. [min]	T/M	T/H	T/L	T/K	T/M	T/H	T/L	T/K
55	8.96 ± 2.58	2.59 ± 0.45	1.84 ± 1.42	0.47 ± 0.16	14.78 ± 6.86	3.93 ± 0.81	2.25 ± 0.41	0.22 ± 0.05
75	11.55 ± 6.25	3.42 ± 0.58	1.84 ± 1.55	0.59 ± 0.26	18.06 ± 5.99	6.24 ± 1.79	2.45 ± 0.36	0.22 ± 0.05
95	14.49 ± 5.17	3.72 ± 0.60	2.05 ± 1.86	0.67 ± 0.41	24.84 ± 11.17	6.11 ± 2.50	2.37 ± 0.41	0.19 ± 0.05

T/M = tumor-to-muscle ratio; T/H = tumor-to-heart ratio; T/L = tumor-to-liver ratio; T/K = tumor-to-kidney ratio.

exhibiting significantly enhanced binding avidities to the GRP receptor compared to the respective monomers.

Moreover, in initial preclinical *in vivo* experiments, the most potent bivalent compound showed improved *in vivo* pharmacokinetic properties compared to not only the monomeric gold standard, but also other bombesin analog dimers described before.

Beyond these findings, it could be shown that binding affinities can surely give a valid indication of biological potency of peptide multimers, but multivalency itself is also contributing to

dx.doi.org/10.1021/bc4004662 | *Bioconjugate Chem.* 2014, 25, 489−500

improved *in vivo* pharmacokinetics as well as tumor accumulation properties.

MATERIALS AND METHODS

General. All commercially available chemicals were of analytical grade and were used without further purification. Resins for peptide synthesis, coupling reagents, and Fmoc-protected amino acids were purchased from NovaBiochem. Fmoc-NH-dPEG(4)-COOH (PEG = polyethyleneglycol) and Fmoc-NH-dPEG(8)-COOH were obtained from Iris Biotech (PEG1820 and PEG1830). Maleimide-NODAGA and tris-*t*Bu-DOTA (NODAGA = 1,4,7-triazacyclononane-1-glutaric acid-4,7-diacetic acid and DOTA = 1,4,7,10-tetraaza-cyclododecane-1,4,7,10-tetraacetic acid) were purchased from CheMatech. ^{125}I-Tyr^4-bombesin was purchased from Perkin−Elmer (NEX258010UC). PAMAM dendrimer scaffolds were synthesized as described previously.[31]

RPMI 1640 medium, fetal bovine serum, and L-glutamine were purchased from PAA, GlutaMax I medium was purchased from Gibco, Dulbecco's phosphate buffered saline (PBS, D8537), and bovine serum albumin was obtained from SigmaAldrich.

For analytical and semipreparative HPLC chromatography, an Agilent 1200 system was used together with a Chromolith Performance (RP-18e, 100−4.6 mm, Merck, Germany) and a Chromolith (RP-18e, 100−10 mm, Merck, Germany) column, operated with flows of 4 and 8 mL/min, respectively. ESI (Electrospray Ionization) and MALDI (Matrix-Assisted Laser Desorption/Ionization) spectra were obtained with a Finnigan MAT95Q and Bruker Daltonics Microflex and Bruker Daltonics Autoflex II spectrometers, respectively. The γ-counter used was a Packard Cobra Quantum.

General Synthesis of PESIN Derivatives 1−3. The peptide derivatives were synthesized on solid support by standard Fmoc solid-phase peptide synthesis using a standard commercially available Rink amide resin, N_α-Fmoc-amino acids, and Fmoc-N_ω-PEG-amino acids. The resulting PEG_X- and cysteine-modified peptides were cleaved from the solid support using a mixture of TFA (trifluoroacetic acid):TIS (triisopropylsilane):H_2O (95:2.5:2.5) for 60 min, suspended in diethyl ether and purified by semipreparative HPLC. The products were isolated as white solids after lyophilization. Gradients used for HPLC purification and synthesis yields for each compound are given below.

1: gradient: 0−40% MeCN + 0.1% FA (formic acid) in 8 min, yield: 60% (58.1 mg), ESI-MS (m/z) for $[M+H^+]^+$ (calculated): 1290.63 (1290.63); $[M+2H^+]^{2+}$ (calculated): 645.82 (645.82). **2**: gradient: 10−50% MeCN + 0.1% FA in 6 min, yield: 44% (34.1 mg), ESI-MS (m/z) for $[M+H^+]^+$ (calculated): 1537.78 (1537.77); $[M+2H^+]^{2+}$ (calculated): 769.39 (769.39). **3**: gradient: 0−40% MeOH + 0.1% FA in 8 min, yield: 50% (43.0 mg), ESI-MS (m/z) for $[M+2H^+]^{2+}$ (calculated): 857.44 (857.44).

General Synthesis of Maleimide-Multimers 4−7. The synthesis of PAMAM dendrimers functionalized with maleimido-hexanoic acid was carried out as described previously[31] with some modifications. A solution of PyBOP (Benzotriazole-1-yl-oxy-*tris*-pyrrolidino-phosphonium hexafluorophosphate) (3.9 equiv per amine function of the respective dendrimer) and DIPEA (*N*,*N*-Diisopropylethylamine) (4 equiv per amine function) in DMF (300 μL) was added to maleimido-hexanoic acid (4 equiv per amine function) and reacted for 2 min. Subsequently, this mixture was added to a solution of the respective PAMAM dendrimer (50 μmol) in DMF (200 μL). After one hour, the volatile components were evaporated and the residue dissolved in H_2O:MeCN 1:2 + 0.1% FA (750 μL). The products were subsequently purified via semipreparative HPLC and lyophilized. Gradients used for HPLC purification and synthesis yields for each substance are given below. The results of characterization complied with those obtained earlier.[31]

4: gradient: 35−90% MeCN + 0.1% FA in 6 min, yield: 64% (17.0 mg). **5**: gradient: 20−90% MeCN + 0.1% FA in 6 min, yield: 47% (10.5 mg). **6**: gradient: 35−65% MeOH + 0.1% FA in 6 min, yield: 67% (18.1 mg). **7**: gradient: 0−60% MeCN + 0.1% FA in 6 min, yield: 46% (11.8 mg).

General Synthesis of *S*-Trityl-Protected PESIN-Multimers 8−19. To a solution of the respective maleimide-multimer (**4**−**7**, 1−12 μmol) in MeCN (500 μL) was added a solution of the respective PESIN-PEG_x-SH (1.2 equiv for monomers, 1.25 equiv for dimers and tetramers, and 1.5 equiv for octamers) in phosphate buffer (PB, 0.1 M, pH 4, 300 μL). The reaction was started by adjusting the pH of the solution to 6.9−7.2 by addition of PB (0.5 M, pH 7.5, 25−50 μL) and monitored by analytical HPLC, being finished within 2−60 min (depending on multimer size) at ambient temperature. The products were purified by semipreparative HPLC and obtained as white solids after lyophilization. Gradients used for HPLC purification, synthesis yields, and characterization data for each substance are given below. Octamers **17**−**19** were not characterized but directly reacted further with maleimide-NODAGA.

8: reaction time: 2 min, gradient: 20−70% MeCN + 0.1% FA in 6 min, yield: 81% (11.8 mg), ESI-MS (m/z) for $[M+2H^+]^{2+}$ (calculated): 1033.98 (1034.00). **9**: reaction time: 2 min, gradient: 20−70% MeCN + 0.1% FA in 6 min, yield: 82% (13.4 mg), ESI-MS (m/z) for $[M+2H^+]^{2+}$ (calculated): 1157.58 (1157.57); $[M+H^++Na^+]^{2+}$ (calculated): 1168.57 (1168.57); $[M+2Na-2H]^{2-}$ (calculated): 1178.57 (1178.56). **10**: reaction time: 2 min, gradient: 20−70% MeCN + 0.1% FA in 6 min, yield: 87% (15.3 mg), ESI-MS (m/z) for $[M+2H^+]^{2+}$ (calculated): 1245.63 (1245.62); $[M+H^++Na^+]^{2+}$ (calculated): 1256.62 (1256.62); $[M-2H]^{2-}$ (calculated): 1243.62 (1243.62); $[M+Na+K]^{2-}$ (calculated): 1274.62 (1274.60). **11**: reaction time: 10 min, gradient: 10−65% MeCN + 0.1% FA in 6 min, yield: 78% (8.6 mg), ESI-MS (m/z) for $[M+4H^+]^{4+}$ (calculated): 945.22 (945.22); $[M+5H^+]^{5+}$ (calculated): 756.38 (756.37). **12**: reaction time: 10 min, gradient: 10−65% MeCN + 0.1% FA in 6 min, yield: 86% (10.7 mg), ESI-MS (m/z) for $[M+4H^+]^{4+}$ (calculated): 1068.79 (1068.79); $[M+5H^+]^{5+}$ (calculated): 855.24 (855.23). **13**: reaction time: 10 min, gradient: 10−65% MeCN + 0.1% FA in 6 min, yield: 87% (11.8 mg), ESI-MS (m/z) for $[M+4H^+]^{4+}$ (calculated): 1156.85 (1156.84); $[M+5H^+]^{5+}$ (calculated): 925.68 (925.67). **14**: reaction time: 25 min, gradient: 10−60% MeCN + 0.1% FA in 6 min, yield: 76% (9.4 mg), ESI-MS (m/z) for $[M+5H^+]^{5+}$ (calculated): 1440.73 (1440.71); $[M+7H^+]^{7+}$ (calculated): 1029.37 (1029.37); $[M+8H^+]^{8+}$ (calculated): 900.83 (900.82). **15**: reaction time: 25 min, gradient: 10−60% MeCN + 0.1% FA in 6 min, yield: 79% (11.1 mg), ESI-MS (m/z) for $[M+8H^+]^{8+}$ (calculated): 1024.40 (1024.39); $[M+9H^+]^{9+}$ (calculated): 910.69 (910.68). **16**: reaction time: 25 min, gradient: 0−50% MeCN + 0.1% FA in 6 min, yield: 74% (11.3 mg), ESI-MS (m/z) for $[M+8H^+]^{8+}$ (calculated): 1112.45 (1112.45); $[M+9H^+]^{9+}$ (calculated): 988.96 (988.95). **17**: reaction time: 60 min, gradient: 0−50% MeCN + 0.1% TFA in 6 min, yield: 73% (8.3 mg). **18**: reaction time: 60 min, gradient: 5−55% MeCN + 0.1% TFA in 6 min, yield: 76% (9.8 mg). **19**: reaction time: 60 min, gradient: 5−55% MeCN + 0.1% TFA in 6 min, yield: 78% (10.9 mg).

dx.doi.org/10.1021/bc4004662 | *Bioconjugate Chem.* 2014, 25, 489−500

General Synthesis of NODAGA-Modified PESIN-Multimers 20−31. To the respective *S*-Trityl-protected PESIN-multimer (**8**−**19**, 0.9−10.7 μmol) was added a mixture of trifluoroacetic acid (TFA, 2 mL) and triisopropylsilane (TIS, 50 μL) and reacted for 5 min at ambient temperature. The volatile components of the mixture were evaporated, the residue dissolved in H_2O:MeCN 1:1 (500−750 μL) and added to solid maleimide-NODAGA (10 mg, 13.3 μmol). The pH of the solution was adjusted to 6.9−7.2 by addition of PB (0.5M, pH 7.5, 125−250 μL) to start the conjugation reaction which was finished within 2−10 min at ambient temperature. The products were purified by semipreparative HPLC and obtained as white solids after lyophilization. Gradients used for HPLC purification, synthesis yields, and characterization data for each substance are given below.

20: gradient: 10−50% MeCN + 0.1% FA in 6 min, yield: 78% (10.3 mg), ESI-MS (*m*/*z*) for $[M+2H^+]^{2+}$ (calculated): 1162.56 (1161.55); $[M+3H^+]^{3+}$ (calculated): 774.71 (774.70); $[M+Na+2H^+]^{3+}$ (calculated): 782.03 (782.03); $[M-2H^+]^{2-}$ (calculated): 1159.55 (1159.55). **21**: gradient: 10−50% MeCN + 0.1% FA in 6 min, yield: 79% (11.9 mg), ESI-MS (*m*/*z*) for $[M+2H^+]^{2+}$ (calculated): 1285.13 (1285.12); $[M+3H^+]^{3+}$ (calculated): 857.09 (857.08); $[M+Na+2H^+]^{3+}$ (calculated): 864.42 (864.41); $[M-2H^+]^{2-}$ (calculated): 1283.12 (1283.12). **22**: gradient: 10−50% MeCN + 0.1% FA in 6 min, yield: 78% (13.2 mg), ESI-MS (*m*/*z*) for $[M+3H^+]^{3+}$ (calculated): 915.79 (915.78); $[M+Na+2H^+]^{3+}$ (calculated): 923.12 (923.11); $[M-2H^+]^{2-}$ (calculated): 1371.17 (1371.18). **23**: gradient: 10−50% MeCN + 0.1% FA in 6 min, yield: 68% (6.3 mg), ESI-MS (*m*/*z*) for $[M+4H^+]^{4+}$ (calculated): 1009.00 (1008.99); $[M+K+Na+2H^+]^{4+}$ (calculated): 1024.23 (1023.98); $[M+K+2Na+H^+]^{4+}$ (calculated): 1029.72 (1029.48); $[M-3H^+]^{3-}$ (calculated): 1342.99 (1342.99). **24**: gradient: 10−50% MeCN + 0.1% FA in 6 min, yield: 63% (7.2 mg), ESI-MS (*m*/*z*) for $[M+5H^+]^{5+}$ (calculated): 906.26 (906.25); $[M+Na+4H^+]^{5+}$ (calculated): 910.65 (910.65); $[M+K+Na+3H^+]^{5+}$ (calculated): 918.24 (918.24); $[M+K+2Na+2H^+]^{5+}$ (calculated): 922.64 (922.64); $[M-3H^+]^{3-}$ (calculated): 1507.74 (1507.75). **25**: gradient: 10−50% MeCN + 0.1% FA in 6 min, yield: 67% (8.2 mg), ESI-MS (*m*/*z*) for $[M+4H^+]^{4+}$ (calculated): 1220.62 (1220.61); $[M+Na+3H^+]^{4+}$ (calculated): 1226.12 (1226.11); $[M+K+Na+2H^+]^{4+}$ (calculated): 1235.60 (1235.60); $[M+K+2Na+H^+]^{4+}$ (calculated): 1241.10 (1241.10); $[M+5H^+]^{5+}$ (calculated): 976.70 (976.69); $[M+K+4H^+]^{5+}$ (calculated): 984.29 (984.28); $[M+K+Na+3H^+]^{5+}$ (calculated): 988.68 (988.68); $[M+K+2Na+2H^+]^{5+}$ (calculated): 993.08 (993.08). **26**: gradient: 10−50% MeCN + 0.1% FA in 6 min, yield: 54% (5.2 mg), ESI-MS (*m*/*z*) for $[M+K+5H^+]^{6+}$ (calculated): 1249.61 (1249.61); $[M+K+Na+4H^+]^{6+}$ (calculated): 1253.27 (1253.27). **27**: gradient: 10−50% MeCN + 0.1% FA in 6 min, yield: 56% (6.3 mg), ESI-MS (*m*/*z*) for $[M+K+Na+5H^+]^{7+}$ (calculated): 1215.60 (1215.60). **28**: gradient: 10−50% MeCN + 0.1% FA in 6 min, yield: 54% (6.3 mg), ESI-MS (*m*/*z*) for $[M+K+5H^+]^{6+}$ (calculated): 1531.78 (1531.77); $[M+K+Na+4H^+]^{6+}$ (calculated): 1535.43 (1535.44); $[M+K+2Na+3H^+]^{6+}$ (calculated): 1539.10 (1539.10); $[M+K+6H^+]^{7+}$ (calculated): 1313.10 (1313.09); $[M+K+Na+5H^+]^{7+}$ (calculated): 1316.24 (1316.23). **29**: gradient: 10−50% MeCN + 0.1% FA in 6 min, yield: 55% (4.6 mg), ESI-MS (*m*/*z*) for $[M+K+7H^+]^{8+}$ (calculated): 1792.89 (1792.88); $[M+K+Na+6H^+]^{8+}$ (calculated): 1795.65 (1795.63); $[M+K+2Na+5H^+]^{8+}$ (calculated): 1798.39 (1798.38), MALDI-MS (*m*/*z*) for $[M+2K]^+$ (calculated): 14,374.7 (14,375.0). **30**: gradient: 10−50% MeCN + 0.1% FA in 6 min, yield: 62% (6.1 mg), MALDI-MS (*m*/*z*) for $[M+3Na]^+$ (calculated): 16,348.7 (16,343.2); $[M+2K]^+$ (calculated): 16,352.2 (16,352.2). **31**: gradient: 10−50% MeCN + 0.1% FA in 6 min, yield: 45% (5.0 mg), MALDI-MS (*m*/*z*) for $[M+H]^+$ (calculated): 17,685.4 (17,683.1); $[M+K]^+$ (calculated): 17,725.7 (17,722.1).

Synthesis of DOTA-PESIN. The peptide was synthesized on solid support by standard Fmoc solid-phase peptide synthesis using a standard commercially available Rink amide resin, N_α-Fmoc-amino acids, Fmoc-NH-dPEG(4)-COOH, and tris-*t*Bu-DOTA. The product was cleaved from the solid support using a mixture of TFA (trifluoroacetic acid):TIS (triisopropylsilane):-H_2O (95:2.5:2.5) for 120 min, suspended in diethyl ether, and purified by semipreparative HPLC. The product was isolated as white solid after lyophilization. A gradient of 0−40% MeCN + 0.1% TFA in 8 min used for HPLC purification and the product was obtained in 18% yields (5.8 mg). MALDI-MS (*m*/*z*) for $[M+H^+]^+$ (calculated): 1574.17 (1573.80); $[M+Na]^+$ (calculated): 1596.79 (1595.78); $[M+K]^+$ (calculated): 1612.05 (1611.75); $[M+2Na]^+$ (calculated): 1617.12 (1617.76).

^{68}Ga-Radiolabeling of NODAGA-Modified PESIN-Multimers 20−31 for *in Vitro* Evaluations. A solution of the respective PESIN multimer (10−12.5 nmol) in HEPES (4-(2-Hydroxyethyl)piperazine-1-ethanesulfonic acid, *N*-(2-Hydroxyethyl)piperazine-*N*′-(2-ethane-sulfonic acid)) buffer (0.025 M, pH 4.0, 50−100 μL) was added to 170−290 MBq of $^{68}Ga^{3+}$ in a solution obtained by fractioned elution of a $^{68}Ge/^{68}Ga$ generator (IGG100, Eckert & Ziegler, Berlin, Germany) with HCl (0.1M, 1.2 mL) and subsequent titration to pH 3.5−4.0 by addition of sodium acetate solution (1.25 M, 90−95 μL). After reaction for 10 min at ambient temperature, the reaction mixtures were analyzed by analytical radio-HPLC. The radiolabeled products were found to be 96−99% pure and obtained in specific activities of 18.9−27.7 GBq/μmol (non-optimized).

Determination of Serum Stability. NODAGA-derivatized PESIN tetramer **26** was radiolabeled with 290 MBq ^{68}Ga as described before and 100 μL of the product solution were added to 500 μL of human serum and incubated at 37 °C. At different time-points, aliquots of 50 μL of the mixture were added to 50 μL of ethanol and the precipitation of serum proteins was enhanced by ice-cooling for 2 min. Supernatant and precipitate were measured for radioactivity. After centrifugation, the supernatant was analyzed by analytical radio-HPLC.

Cell Culture. PC-3 prostate adenocarcinoma cells were grown in RPMI 1640 medium, supplemented with 10% (v/v) fetal bovine serum and 1% (v/v) L-glutamine, at 37 °C in a humidified CO_2 (5%) atmosphere.

Cell Binding Assay. In vitro binding affinities were measured via competitive displacement experiments using a Millipore Multiscreen punch kit. Millipore 96-well filter plates were incubated with 200 μL per well with Dulbecco's phosphate buffered saline (PBS, modified, without $CaCl_2$ and $MgCl_2$, sterile-filtered, Sigma, supplemented with 1 g/100 mL bovine serum albumin) for one hour before use. PC-3 cells were harvested, suspended in Opti-MEM I (Gibco, GlutaMax I), and seeded in 96-well plates at 10^5 cells per well. Subsequently, the cells were incubated on a shaker for one hour at ambient temperature with 0.1 nM ^{125}I-[Tyr^4]-bombesin (81.4 GBq/μmol) as the GRPR-specific radioligand in the presence of increasing concentrations (0−10 μM) of competing PESIN multimers **20**−**31** in a total volume of 100 μL. After incubation, the cell pellets were washed 3 times (2 × 100 μL and 1 × 200 μL) with Dulbecco's phosphate buffered saline (PBS) using the

dx.doi.org/10.1021/bc4004662 | *Bioconjugate Chem.* 2014, 25, 489−500

Millipore Multiscreen vacuum manifold for filtration. The filters were collected and measured for radioactivity in the γ-counter. Experiments were done at least three times; each experiment was carried out in triplicate. The 50% inhibitory concentration (IC_{50}) values were calculated by fitting the data with nonlinear regression analysis using the software GraphPad Prism (v 5.03) and compared to natural bombesin.

^{68}Ga-Radiolabeling of [^{68}Ga]23 and ^{68}Ga-DOTA-PESIN and Their *in Vivo* Evaluation in PC-3 Tumor-Bearing Mice. PET Study: All animal experiments were performed in compliance with the German animal protection laws and protocols of the local committee. Twelve male nude mice (SCID, 25−30 g) were subcutaneously injected with PC-3 cells (5×10^6 cells/mouse) into the right flank. After cell inoculation, the tumors were allowed to grow for 6 to 8 weeks. For animal PET imaging, 10 MBq of the respective radiotracer were injected via the lateral tail vain under isoflurane anesthesia. In the case of blocking experiments, the animals were injected with cold bombesin (100 μg) prior to injection of the radiotracer. Dynamic animal PET images were acquired over 120 min using a Siemens Inveon P120 Dedicated PET system (Siemens Preclinical Imaging, Knoxville, TN, USA). Data were divided into time frames from 10 s to 10 min for the assessment of temporal changes in regional tracer accumulation. The images were reconstructed using an OSEM3D/MAP algorithm. Regions of interest (ROIs) were defined for the quantification of tracer accumulation in different tissues.

^{68}Ga-radiolabeling of DOTA-PESIN: A solution of DOTA-PESIN (10 nmol) in water (10 μL) was added to ∼800 MBq of $^{68}Ga^{3+}$ in a solution obtained by fractioned elution of a ^{68}Ge/^{68}Ga generator (ITG, Garching, Germany) with HCl (0.05 M, 2.5 mL) and subsequent titration to pH 4.3 by addition of sodium acetate solution (1 M, 180 μL). After reaction for 10 min at 105 °C, the solution was neutralized with HEPES buffer (2 M, pH 8, 320 μL). The radiochemical yields and purities were assessed by analytical radio-HPLC. The product was obtained in ≥96% radiochemical purity and in specific activities of 76−79 GBq/μmol (nonoptimized).

^{68}Ga-radiolabeling of **23**: A solution of **23** (20 nmol) in HEPES buffer (0.025 M, pH 4) was added to ∼800 MBq of $^{68}Ga^{3+}$ in a solution obtained by fractioned elution of a ^{68}Ge/^{68}Ga generator (ITG, Garching, Germany) with HCl (0.05 M, 2.5 mL) and subsequent titration to pH 4.4 by addition of sodium acetate solution (1 M, 200 μL). After reaction for 10 min at ambient temperature, the solution was neutralized with HEPES buffer (2 M, pH 8, 300 μL). The radiochemical yields and purities were assessed by analytical radio-HPLC. The product was obtained in ≥96% radiochemical purity and in specific activities of 38−39 GBq/μmol (nonoptimized).

AUTHOR INFORMATION

Corresponding Author

*E-mail: Carmen.Waengler@medma.uni-heidelberg.de. Phone: +49 (0)621 383 3761; fax: +49 (0)621 383 1910.

Notes

The authors declare no competing financial interest.

ACKNOWLEDGMENTS

The authors would like to thank Dr. Werner Spahl for his help with ESI mass spectrometry and Prof. Dr. Carell for granting access to his MALDI spectrometer (both from Department of Organic Chemistry, Ludwig-Maximilians University Munich, Germany). Financial support was granted by the *Fonds der Chemischen Industrie* and the *BMBF* (German Federal Ministry of Education and Research) Leading Edge Cluster "m^4 − Personalized Medicine and Targeted Therapies" which is gratefully acknowledged.

REFERENCES

(1) Reubi, J. C., Wenger, S., Schmuckli-Maurer, J., Schaer, J. C., and Gugger, M. (2002) Bombesin receptor subtypes in human cancers: Detection with the universal radioligand I-125-[D-TYR6, beta-ALA(11), PHE13, NLE14] bombesin(6−14). *Clin. Cancer Res. 8*, 1139−1146.

(2) Cornelio, D. B., Roesler, R., and Schwartsmann, G. (2007) Gastrin-releasing peptide receptor as a molecular target in experimental anticancer therapy. *Ann. Oncol. 18*, 1457−1466.

(3) Ambrosini, V., Fani, M., Fanti, S., Forrer, F., and Maecke, H. R. (2011) Radiopeptide imaging and therapy in europe. *J. Nucl. Med. 52*, 42s−55s.

(4) Liu, S. (2009) Radiolabeled cyclic RGD peptides as integrin alpha(v)beta(3)-targeted radiotracers: maximizing binding affinity via bivalency. *Bioconjugate Chem. 20*, 2199−2213.

(5) Reubi, J. C., and Maecke, H. R. (2008) Peptide-based probes for cancer imaging. *J. Nucl. Med. 49*, 1735−1738.

(6) Reubi, J. C., Macke, H. R., and Krenning, E. P. (2005) Candidates for peptide receptor radiotherapy today and in the future. *J. Nucl. Med. 46*, 67s−75s.

(7) Ananias, H. J., de Jong, I. J., Dierckx, R. A., van de Wiele, C., Helfrich, W., and Elsinga, P. H. (2008) Nuclear imaging of prostate cancer with gastrin-releasing-peptide-receptor targeted radiopharmaceuticals. *Curr. Pharm. Des. 14*, 3033−3047.

(8) Cescato, R., Maina, T., Nock, B., Nikolopoulou, A., Charalambidis, D., Piccand, V., and Reubi, J. C. (2008) Bombesin receptor antagonists may be preferable to agonists for tumor targeting. *J. Nucl. Med. 49*, 318−326.

(9) Mansi, R., Wang, X. J., Forrer, F., Kneifel, S., Tamma, M. L., Waser, B., Cescato, R., Reubi, J. C., and Maecke, H. R. (2009) Evaluation of a 1,4,7,10-tetraazacyclododecane-1,4,7,10-tetraacetic acid-conjugated bombesin-based radioantagonist for the labeling with single-photon emission computed tomography, positron emission tomography, and therapeutic radionuclides. *Clin. Cancer Res. 15*, 5240−5249.

(10) Mansi, R., Wang, X. J., Forrer, F., Waser, B., Cescato, R., Graham, K., Borkowski, S., Reubi, J. C., and Maecke, H. R. (2011) Development of a potent DOTA-conjugated bombesin antagonist for targeting GRPr-positive tumours. *Eur. J. Nucl. Med. Mol. Imaging 38*, 97−107.

(11) Abiraj, K., Mansi, R., Tamma, M. L., Fani, M., Forrer, F., Nicolas, G., Cescato, R., Reubi, J. C., and Maecke, H. R. (2011) Bombesin antagonist-based radioligands for translational nuclear imaging of gastrin-releasing peptide receptor-positive tumors. *J. Nucl. Med. 52*, 1970−1978.

(12) Lane, S. R., Nanda, P., Rold, T. L., Sieckman, G. L., Figueroa, S. D., Hoffman, T. J., Jurisson, S. S., and Smith, C. J. (2010) Optimization, biological evaluation and microPET imaging of copper-64-labeled bombesin agonists, [Cu-64-NO_2A-(X)-BBN(7−14)NH_2], in a prostate tumor xenografted mouse model. *Nucl. Med. Biol. 37*, 751−761.

(13) Höhne, A., Mu, L., Honer, M., Schubiger, P. A., Ametamey, S. M., Graham, K., Stellfeld, T., Borkowski, S., Berndorff, D., Klar, U., Voigtmann, U., Cyr, J. E., Friebe, M., Dinkelborg, L., and Srinivasan, A. (2008) Synthesis, F-18-labeling, and in vitro and in vivo studies of bombesin peptides modified with silicon-based building blocks. *Bioconjugate Chem. 19*, 1871−1879.

(14) Honer, M., Mu, L. J., Stellfeld, T., Graham, K., Martic, M., Fischer, C. R., Lehmann, L., Schubiger, P. A., Ametamey, S. M., Dinkelborg, L., Srinivasan, A., and Borkowski, S. (2011) F-18-labeled bombesin analog for specific and effective targeting of prostate tumors expressing gastrin-releasing peptide receptors. *J. Nucl. Med. 52*, 270−278.

(15) Nanda, P. K., Pandey, U., Bottenus, B. N., Rold, T. L., Sieckman, G. L., Szczodroski, A. F., Hoffman, T. J., and Smith, C. J. (2012)

Bombesin analogues for gastrin-releasing peptide receptor imaging. *Nucl. Med. Biol. 39*, 461−471.
(16) Fournier, P., Dumulon-Perreault, V., Ait-Mohand, S., Tremblay, S., Benard, F., Lecomte, R., and Guerin, B. (2012) Novel radiolabeled peptides for breast and prostate tumor PET imaging: Cu-64/and Ga-68/NOTA-PEG-[D-Tyr(6),beta Ala(11),Thi(13),Nle(14)]BBN(6−14). *Bioconjugate Chem. 23*, 1687−1693.
(17) Schroeder, R. P. J., Muller, C., Reneman, S., Melis, M. L., Breeman, W. A. P., de Blois, E., Bangma, C. H., Krenning, E. P., van Weerden, W. M., and de Jong, M. (2010) A standardised study to compare prostate cancer targeting efficacy of five radiolabelled bombesin analogues. *Eur. J. Nucl. Med. Mol. Imaging 37*, 1386−1396.
(18) Wild, D., Frischknecht, M., Zhang, H. W., Morgenstern, A., Bruchertseifer, F., Boisclair, J., Provencher-Bolliger, A., Reubi, J. C., and Maecke, H. R. (2011) Alpha- versus beta-particle radiopeptide therapy in a human prostate cancer model (Bi-213-DOTA-PESIN and Bi-213-AMBA versus Lu-177-DOTA-PESIN). *Cancer Res. 71*, 1009−1018.
(19) Zhang, H. W., Schuhmacher, J., Waser, B., Wild, D., Eisenhut, M., Reubi, J. C., and Maecke, H. R. (2007) DOTA-PESIN, a DOTA-conjugated bombesin derivative designed for the imaging and targeted radionuclide treatment of bombesin receptor-positive tumours. *Eur. J. Nucl. Med. Mol. Imaging 34*, 1198−1208.
(20) Lears, K. A., Ferdani, R., Liang, K. X., Zheleznyak, A., Andrews, R., Sherman, C. D., Achilefu, S., Anderson, C. J., and Rogers, B. E. (2011) In vitro and in vivo evaluation of Cu-64-labeled SarAr-bombesin analogs in gastrin-releasing peptide receptor-expressing prostate cancer. *J. Nucl. Med. 52*, 470−477.
(21) Wu, Z. H., Li, Z. B., Chen, K., Cai, W. B., He, L., Chin, F. T., Li, F., and Chen, X. Y. (2007) MicroPET of tumor integrin alpha(v)beta(3) expression using F-18-labeled PEGylated tetrameric RGD peptide (F-18-FPRGD4). *J. Nucl. Med. 48*, 1536−1544.
(22) Liu, S., Liu, Z., Chen, K., Yan, Y., Watzlowik, P., Wester, H. J., Chin, F. T., and Chen, X. (2010) ^{18}F-labeled galacto and PEGylated RGD dimers for PET imaging of alphavbeta3 integrin expression. *Mol. Imaging Biol. 12*, 530−538.
(23) Dijkgraaf, I., Yim, C. B., Franssen, G. M., Schuit, R. C., Luurtsema, G., Liu, S. A., Oyen, W. J. G., and Boerman, O. C. (2011) PET imaging of alpha(v)beta(3) integrin expression in tumours with Ga-68-labelled mono-, di- and tetrameric RGD peptides. *Eur. J. Nucl. Med. Mol. Imaging 38*, 128−137.
(24) Fournier, P., Dumulon-Perreault, V., Ait-Mohand, S., Langlois, R., Benard, F., Lecomte, R., and Guerin, B. (2012) Comparative study of ^{64}Cu/NOTA-[D-Tyr6,betaAla11,Thi13,Nle14]BBN(6−14) monomer and dimers for prostate cancer PET imaging. *EJNMMI Res. 2*, 8.
(25) Yu, Z., Carlucci, G., Ananias, H. J., Dierckx, R. A., Liu, S., Helfrich, W., Wang, F., de Jong, I. J., and Elsinga, P. H. (2013) Evaluation of a technetium-99m labeled bombesin homodimer for GRPR imaging in prostate cancer. *Amino Acids 44*, 543−553.
(26) Abiraj, K., Jaccard, H., Kretzschmar, M., Helm, L., and Maecke, H. R. (2008) Novel DOTA-based prochelator for divalent peptide vectorization: synthesis of dimeric bombesin analogues for multi-modality tumor imaging and therapy. *Chem. Commun. 28*, 3248−3250.
(27) Gawlak, S. L., Kiener, P. A., Braslawsky, G. R., and Greenfield, R. S. (1991) Homodimeric forms of bombesin act as potent antagonists of bombesin on Swiss 3T3 cells. *Growth Factors 5*, 159−170.
(28) Carrithers, M. D., and Lerner, M. R. (1996) Synthesis and characterization of bivalent peptide ligands targeted to G-protein-coupled receptors. *Chem. Biol. 3*, 537−542.
(29) Carlucci, G., Ananias, H. J. K., Yu, Z., Hoving, H. D., Helfrich, W., Dierckx, R. A. J. O., Liu, S., de Jong, I. J., and Elsinga, P. H. (2013) Preclinical evaluation of a novel In-111-labeled bombesin homodimer for improved imaging of GRPR-positive prostate cancer. *Mol. Pharmaceutics 10*, 1716−1724.
(30) Hultsch, C., Pawelke, B., Bergmann, R., and Wuest, F. (2006) Synthesis and evaluation of novel multimeric neurotensin(8−13) analogs. *Bioorg. Med. Chem. 14*, 5913−5920.
(31) Wängler, C., Moldenhauer, G., Eisenhut, M., Haberkorn, U., and Mier, W. (2008) Antibody-dendrimer conjugates: the number, not the size of the dendrimers, determines the immunoreactivity. *Bioconjugate Chem. 19*, 813−820.
(32) Li, Z. B., Cai, W. B., Cao, Q. Z., Chen, K., Wu, Z. H., He, L. N., and Chen, X. Y. (2007) ^{64}Cu-labeled tetrameric and octameric RGD peptides for small-animal PET of tumor alpha(v)beta(3) integrin expression. *J. Nucl. Med. 48*, 1162−1171.
(33) Wu, Y., Cai, W. B., and Chen, X. Y. (2006) Near-infrared fluorescence imaging of tumor integrin alpha(v)beta(3) expression with Cy7-labeled RGD multimers. *Mol. Imaging Biol. 8*, 226−236.
(34) Chen, X. Y., Liu, S., Hou, Y. P., Tohme, M., Park, R., Bading, J. R., and Conti, P. S. (2004) MicroPET imaging of breast cancer alpha(v)-integrin expression with Cu-64-labeled dimeric RGD peptides. *Mol. Imaging Biol. 6*, 350−359.
(35) Wängler, C., Maschauer, S., Prante, O., Schafer, M., Schirrmacher, R., Bartenstein, P., Eisenhut, M., and Wängler, B. (2010) Multimerization of cRGD peptides by click chemistry: synthetic strategies, chemical limitations, and influence on biological properties. *ChemBioChem 11*, 2168−2181.
(36) Wängler, C., Waser, B., Alke, A., Iovkova, L., Buchholz, H. G., Niedermoser, S., Jurkschat, K., Fottner, C., Bartenstein, P., Schirrmacher, R., Reubi, J. C., Wester, H. J., and Wängler, B. (2010) One-step (18)F-labeling of carbohydrate-conjugated octreotate-derivatives containing a silicon-fluoride-acceptor (SiFA): in vitro and in vivo evaluation as tumor imaging agents for positron emission tomography (PET). *Bioconjugate Chem. 21*, 2289−2296.
(37) Wellings, D. A., and Atherton, E. (1997) Standard Fmoc protocols. *Methods Enzymol. 289*, 44−67.
(38) Persson, M., Madsen, J., Ostergaard, S., Ploug, M., and Kjaer, A. (2012) Ga-68-labeling and in vivo evaluation of a uPAR binding DOTA- and NODAGA-conjugated peptide for PET imaging of invasive cancers. *Nucl. Med. Biol. 39*, 560−569.
(39) Wängler, C., Wängler, B., Lehner, S., Elsner, A., Todica, A., Bartenstein, P., Hacker, M., and Schirrmacher, R. (2011) A universally applicable (68)Ga-labeling technique for proteins. *J. Nucl. Med. 52*, 586−591.
(40) Ait-Mohand, S., Fournier, P., Dumulon-Perreault, V., Kiefer, G. E., Jurek, P., Ferreira, C. L., Benard, F., and Guerin, B. (2011) Evaluation of Cu-64-labeled bifunctional chelate-bombesin conjugates. *Bioconjugate Chem. 22*, 1729−1735.
(41) Zhang, Y., Hong, H., Engle, J. W., Bean, J., Yang, Y. N., Leigh, B. R., Barnhart, T. E., and Cai, W. B. (2011) Positron emission tomography imaging of CD105 expression with a Cu-64-labeled monoclonal antibody: NOTA is superior to DOTA. *PLoS One 6*, e28005.
(42) Breeman, W. A. P., de Jong, M., de Blois, E., Bernard, B. F., Konijnenberg, M., and Krenning, E. P. (2005) Radiolabelling DOTA-peptides with Ga-68. *Eur. J. Nucl. Med. Mol. Imaging 32*, 478−485.
(43) Zhang, X. Z., Xiong, Z. M., Wu, Y., Cai, W. B., Tseng, J. R., Gambhir, S. S., and Chen, X. Y. (2006) Quantitative PET imaging of tumor integrin alpha(v)beta(3) expression with F-18-FRGD2. *J. Nucl. Med. 47*, 113−121.
(44) Yang, Y. S., Zhang, X. Z., Xiong, Z. M., and Chen, X. Y. (2006) Comparative in vitro and in vivo evaluation of two Cu-64-labeled bombesin analogs in a mouse model of human prostate adenocarcinoma. *Nucl. Med. Biol. 33*, 371−380.
(45) Humblet, V., Misra, P., Bhushan, K. R., Nasr, K., Ko, Y. S., Tsukamoto, T., Pannier, N., Frangioni, J. V., and Maison, W. (2009) Multivalent scaffolds for affinity maturation of small molecule cell surface binders and their application to prostate tumor targeting. *J. Med. Chem. 52*, 544−550.
(46) Yim, C. B., van der Wildt, B., Dijkgraaf, I., Joosten, L., Eek, A., Versluis, C., Rijkers, D. T. S., Boerman, O. C., and Liskamp, R. M. J. (2011) Spacer effects on in vivo properties of DOTA-conjugated dimeric [Tyr3] octreotate peptides synthesized by a ″Cu-I-Click″ and ″Sulfo-Click″ ligation method. *ChemBioChem 12*, 750−760.
(47) Dijkgraaf, I., Kruijtzer, J. A. W., Liu, S., Soede, A. C., Oyen, W. J. G., Corstens, F. H. M., Liskamp, R. M. J., and Boerman, O. C. (2007) Improved targeting of the alpha(v)beta(3) integrin by multimerisation of RGD peptides. *Eur. J. Nucl. Med. Mol. Imaging 34*, 267−273.